
CATALYSIS

Photocatalytic Generation of Hydrogen from Organic Substances Using Iron-Containing Composites under the Conditions of UV and Visible Irradiation

L. N. Skvortsova^{a,*}, I. A. Artyukh^a, K. A. Bolgaru^b, and I. A. Pichikov^a

^a National Research Tomsk State University, Tomsk, 634050 Russia

^b Tomsk Scientific Center, Siberian Branch, Russian Academy of Sciences, Tomsk, 634021 Russia

*e-mail: lnskvorcova@inbox.ru

Received November 8, 2019; revised January 22, 2020; accepted February 8, 2020

Abstract—Morphological features of iron-containing composites based on silicon, titanium, vanadium, and boron nitrides and prepared by self-propagating synthesis were examined by scanning electron microscopy, and the content of elements (B, Si, N, Ti, V, O, Fe, C, Al, Mg, Ca) on their surface was quantitatively estimated using an attachment for EDX microanalysis. The optical properties of the composites were studied, and the band gap values for the semiconductors incorporated in the ceramic matrix were determined. A comparative evaluation of the performance of the composites in hydrogen generation from solutions of organic substances (HCOOH , $\text{H}_2\text{C}_2\text{O}_4$, malic acid, sucrose) under UV and visible irradiation was made. The efficiency of the photocatalytic generation of hydrogen under the action of visible light is shown to be associated both with the composition of the ceramic matrix containing semiconductor compounds and with the occurrence of the photo-Fenton process in the solution in the presence of hydrogen peroxide.

Keywords: iron-containing metal–ceramic composites, semiconductors, heterogeneous photocatalysis, homogeneous photocatalysis, hydrogen power engineering

DOI: 10.1134/S1070427220070034

The efficiency of the solar energy utilization in hydrogen generation processes using semiconductor catalysts is yet insufficient. Systems active under visible irradiation are being studied. For example, systems with titanium dioxide [1], absorbing visible light, are being developed. The efficiency of the H_2 generation from water under the action of UV/visible irradiation was significantly enhanced by using metals (Cu, Au, Pt) as TiO_2 cocatalysts [2]. Metal chalcogenides are good materials for photocatalytic generation of hydrogen, because they exhibit activity in the far-UV and visible range. Effective $\text{Bi}_2\text{S}_3/\text{SnS}$ [3] and In/SnS [4] composites for hydrogen generation from water were suggested. Markovskaya et al. [5] developed semiconductor photocatalysts based on nanostructured $\text{ZnS}-\text{CdS}$ solid solutions applied onto a porous support (silica gels, galloisite nanotubes) for the H_2 generation from aqueous solutions of inorganic electron donors ($\text{Na}_2\text{S}/\text{Na}_2\text{SO}_3$) under irradiation with visible light

($\lambda = 450$ nm). Photocatalysts combining several semiconductors, in particular, $\text{CdS}-\text{TiO}_2$ and $\text{SnO}_2-\text{TiO}_2$ [6], show promise for expanding the range of the active light toward visible region.

Iron-containing photo-Fenton process catalysts are of particular interest as economically and environmentally attractive materials. We prepared stable iron-containing catalytic composites by self-propagating high-temperature synthesis in the autowave nitridization of iron alloys. The iron–ceramic materials showed high performance in oxidative degradation of organic contaminants with simultaneous hydrogen evolution under the action of UV irradiation [7].

Previously we demonstrated the possibility of modifying the ceramic matrix of composites based on silicon nitride and SiAlON by introducing into its formulation semiconductor compounds (SiC, TiN) in the synthesis step to enhance the photocatalyst activity and shift it toward the visible range [8]. The composites

Table 1. Characteristics of the composites and separate semiconductors

Composite	Phase composition ^a	E_g , eV	Iron content, wt %
SiN	β-Si₃N₄ , α-Fe, β-Si ₃ Al ₃ O ₃ N ₅ , SiC , Fe _x Si _y	3.1 [11]	1.8–2.6
		2.4 [11]	
TiN	TiN , β-Si ₃ N ₄ , α-Si ₃ N ₄ , α-Fe, Fe _x Si _y	3.3 [11]	2.0–4.7
		5.4	
VN	VN , α-Fe, V ₂ N	3.6	15–19
		5.3	
BN	α-BN , α-Fe, FeB , Fe ₂ B	3.8	5–35
		5.3	

^a Semiconductor phases are printed bold.

showed high performance in H₂ generation in the course of decomposition of sacrificial reagents (H₂C₂O₄, HCOOH, malic acid) under the conditions of UV irradiation.

This study was aimed at comparative evaluation of the photocatalytic activity of modified composites in the course of H₂ generation from sacrificial reagents under the conditions of UV and visible irradiation and at determination of the photocatalytic activity of an iron–ceramic sample based on a wide-band-gap semiconductor, vanadium nitride.

EXPERIMENTAL

Synthesis of the modified composites and analysis of their phase composition were performed at the Department of Structural Macrokinetics, Tomsk Scientific Center, Siberian Branch, Russian Academy of Sciences. The composites were prepared in the autowave heating mode using iron alloys (ferrosilicoaluminum, ferrovanadium, ferroboron) as precursors. To enhance the photocatalytic activity of the materials, the ceramic matrix was modified by introducing semiconductor compounds (SiC, TiN). The procedures for preparing composites based on nitrides by self-propagating high-temperature synthesis are described in [9].

X-ray diffraction analysis of the materials was performed with a Shimadzu XRD6000 diffractometer (Japan) (Table 1). The SiN sample prepared by nitridization of ferrosilicoaluminum with the addition of shungite as modifier consists of the two major phases, β-Si₃N₄ and β-Si₃Al₃O₃N₅ with the prevalence of the silicon nitride phase, and contains also the phases of SiC, α-Fe metal, and intermediate nitridization products, iron silicides Fe_xSi_y. The TiN composite was prepared by nitridization of ferrosilicoaluminum with the addition

of titanium metal. The absence of the SiAlON phase is caused by its dissolution in the crystal lattice of silicon nitride. At 20 wt % dilution of ferrosilicoaluminum with titanium, the TiN phase prevails, and the phases of α-Fe and iron silicides Fe_xSi_y are also present. The VN sample is a product of ferrovanadium nitridization; therefore, its phase composition includes only the synthesis products. The phase composition of the composite based on BN, prepared by the combustion of ferroboron in nitrogen, includes α-BN with the hexagonal lattice, α-Fe, and unchanged ferroboron phases (FeB, Fe₂B). Thus, the ceramic matrices of the composites studied contain wide-band-gap semiconductors (Si₃N₄, SiC, TiN, VN, BN).

The surface morphology was studied with a Hitachi TM3000 scanning electron microscope at an accelerating voltage of 15 kV under the conditions of low vacuum (electron gun: 5 × 10⁻² Pa; sample chamber: 30–50 Pa). Elemental analysis of the materials was performed with a Quantax 70 attachment for EDX microanalysis.

The optical properties of the VN and BN samples were studied with a UV-Visible Evolution 600 spectrophotometer (Thermo Scientific, the United States) using MgO as a reference. We recorded the diffuse reflectance spectra, which were transformed into the electronic absorption spectra using the Kubelka–Munk function [$F = (1 - R)^2/2R$, where R is the diffuse reflection coefficient]. The band gap width was determined from the edge of the main optical absorption band. Then the electronic absorption spectra were transformed in the coordinates absorption coefficient [$F(R)E$]–photon energy ($h\nu$). The quantity E_g was determined by extrapolation of the linear portion of the dependence $[F(R)E]^2/[F(R)E]^{0.5} = f(h\nu)$ to intersection with the $h\nu$ axis.

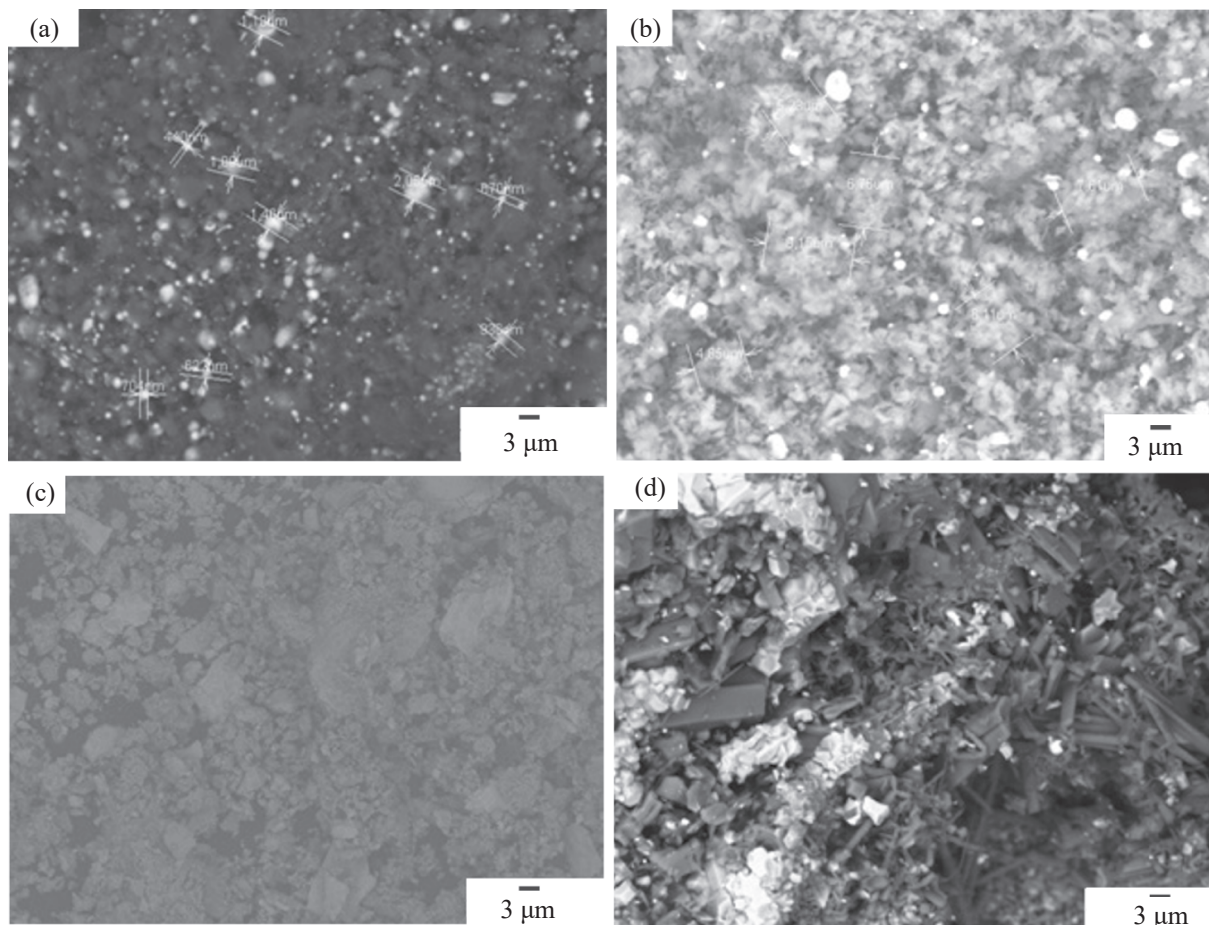


Fig. 1. Electron micrographs of the surface of the composites (a) BN, (b) SiN, (c) VN, and (d) TiN.

A DRL-250 high-pressure mercury lamp with the range 240–1100 nm and the strongest line at 254 nm served as a UV radiation source. A DIORA 30 LED lamp (Fiztekh-Energo, Tomsk, Russia) with the range 410–750 nm and the strongest lines at 450 and 600 nm was used for visible irradiation. The generated hydrogen in the gas mixture of the reaction systems was collected using an installation described in [10].

Photocatalytic generation of hydrogen. A 200-mg portion of the composite was placed in a 100-mL quartz reactor and poured over with 20 mL of a model solution of a sacrificial reagent, after which 0.2 mL of 0.1 M H₂O₂ was added if necessary. The reactor was hermetically sealed and placed on a magnetic stirrer arranged in front of the radiation source. The stirred composite/solution suspension was bubbled with nitrogen from a cylinder prior to irradiation to remove gases adsorbed by the catalyst. In the course of irradiation, nitrogen was fed to the

reactor at a constant rate (10 mL min⁻¹), and the gas mixture at the outlet was fed to the flow meter with a soap solution to monitor the gas flow rate. Samples for analysis were withdrawn into a closable 100-mL gas pipette after its 20-min flushing with a nitrogen–gas mixture. The gas mixture was collected for 10 min and analyzed by gas chromatography with a Kristall 5000-1 device (Khromatek, Russia, 2007), and the catalyst performance in generation of molecular hydrogen was evaluated. The random error did not exceed 10%.

As sacrificial reagents we used aqueous solutions of carboxylic acids (HCOOH, H₂C₂O₄, malic) and sucrose, which proved to be effective in hydrogen generation in the presence of Fe-containing composites under UV irradiation [8].

RESULTS AND DISCUSSION

In the BN sample, light particles of the metal phase of the 0.45–2.1 μm size are concentrated in the center,

Table 2. Comparison of the performance of the composites in H₂ generation from solutions of sacrificial reagents under UV and visible irradiation

System, M	Performance, μmol g ⁻¹ h ⁻¹					
	UV irradiation			visible irradiation		
	SiN	TiN	VN	SiN	TiN	VN
0.5H ₂ C ₂ O ₄ /0.001H ₂ O ₂	755	644	756	660	190	1070
0.5HCOOH/0.001H ₂ O ₂	Not studied	541	561	201	145	759
1% C ₁₂ H ₂₂ O ₁₁ (sucrose), pH 2	276	342	259	157	62	225
0.5HCOOH/0.001H ₂ O ₂ (without composite)		13			11	

and dark particles of boron nitride of the 2–7 μm size are uniformly distributed over the surface (Fig. 1a).

Granules of the SiN and VN composites have a round shape and are agglomerates of particles with the grain size covering a wide range: 1–5 μm for SiN and 1–35 μm for VN (Figs. 1b, 1c). The TiN composite mainly consists of particles in the form of plates and large and small faceted tubes of 2–11 μm size (Fig. 1d). Elemental microanalysis shows that the phase having the shape of faceted tubes is TiN. The iron metal phase is distributed more uniformly over the surface of the SiN and VN composites. Along with the main phase-forming elements, the composites contain impurity elements, in particular, Al, C, Mg, and Ca (Fig. 1).

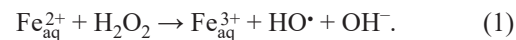
The optical properties of the SiN and TiN composites were studied and described previously [8]. In this study, we recorded the diffuse reflectance spectra of the samples based on boron and vanadium nitrides, which were transformed using the Kubelka–Munk function (Fig. 2).

The composites are characterized by relatively low absorbance in the middle- and near-UV range (280–400 nm) compared to the SiN and TiN samples, for which the $F(R)$ values in this range of the spectrum are 1–1.5 [8]. The absorption band of the BN composite in the region of 250 nm (Fig. 2a) belongs to the unchanged ferroboron. The VN composite absorbs in the near-UV and range and in the range 280–300 nm, which is associated with the presence of the VN and V₂N phases. The electronic absorption spectra were transformed in the coordinates absorption coefficient–photon energy ($h\nu$). Semiconductor compounds present in the BN composite are characterized by direct electron transfer from the valence band (VB) to the conduction band (CB); therefore, to determine the band gap width (E_g),

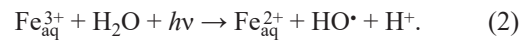
we plotted the dependence $[F(R)E]^2 = f(h\nu)$. Vanadium nitride is an indirect-band-gap superconductor, and we used for it the dependence $[F(R)E]^{0.5} = f(h\nu)$. The band gap width for the semiconductor phases was determined from the edge of the main optical absorption band (Figs. 2b, 2d).

The band gap width in semiconductors (Table 1) present in the ceramic matrix of the composites is smaller than the photon energy of the UV radiation source (4.5 eV). The electronic absorption spectra and the band gap widths of the semiconductor phases of the composites under consideration also suggest that these composites should exhibit activity in the far-UV and visible ranges.

Partial dissolution of iron metal from the sample surface in the presence of H₂O₂ creates the conditions for the occurrence of the photo-Fenton process generating hydroxyl radicals [11, 12]. The classical Fenton process is based on the reaction of hydrogen peroxide with bivalent iron ions in an acid solution; in this process, H₂O₂ is an oxidant and Fe²⁺ is a catalyst. The mechanism of the Fenton process with the generation of hydroxyl radicals is usually presented as follows:



The reaction is accelerated under UV irradiation leading to the conversion of Fe³⁺ ions to Fe²⁺ ions with the release of an additional amount of hydroxyl radicals:



Thus, the hydrogen generation from organic compounds is possible under the conditions combining heterogeneous and homogeneous photocatalysis.

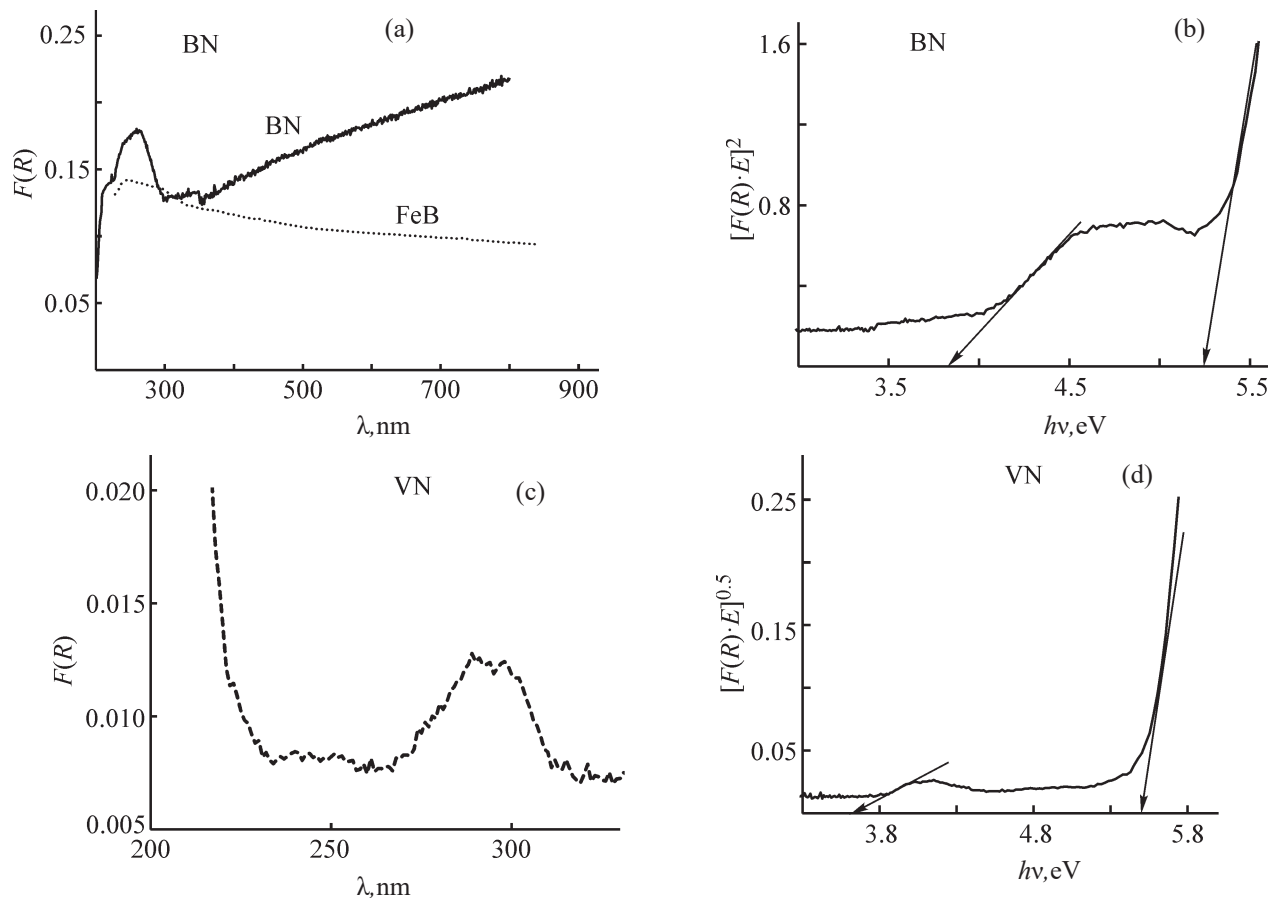
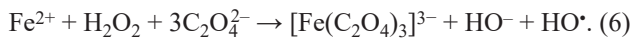
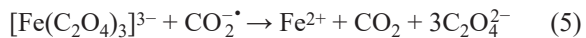
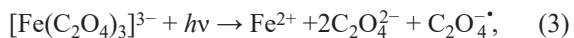


Fig. 2. (a, c) Electronic absorption spectra and (b, d) plots of the absorption coefficients vs. photon energy for the composites (a, b) BN and (c, d) VN.

The highest performance of the catalysts is observed in H₂ generation from oxalic acid solutions with the addition of H₂O₂ (Table 2). In the presence of the VN sample, the efficiency of the H₂ evolution under visible irradiation is considerably higher than under UV irradiation. The composite based on vanadium nitride contains the largest amount of iron (Table 1); its dissolution results in the formation of the photoactive ferrioxalate complex [Fe(C₂O₄)₃]³⁻, which undergoes photolysis in the range 400–500 nm and generates Fe²⁺ and hydroxyl radicals with high quantum yield (1.24) [13]:



According to [14], carboxylic acids are oxidized

with hydroxyl radicals with the release of hydrogen. According to [15], photochemical decomposition of formic acid can occur with the release of CO₂ and H₂. Formic acid remains one of promising sacrificial reagents.

The SiN and TiN composites are characterized by low and virtually equal content of surface iron (Table 1). On the other hand, the sample based on silicon nitride exhibits considerably higher performance in the H₂ generation under visible irradiation in all the systems. This fact suggests the participation of the semiconductor SiC phase ($E_g = 2.4$ eV) in the photolytic process, as this phase absorbs in the region of the most intense radiation of the visible light lamp (450 nm), and the role of the heterogeneous photocatalysis. The fact that the efficiency of the H₂ generation from solutions of sacrificial reagents with the addition of H₂O₂ under UV irradiation differs insignificantly for all the composites also counts in

Table 3. Results of photocatalytic generation of H₂ from solutions of carboxylic acids under visible irradiation with the addition of H₂O₂ and without it

Composite	System, M	Performance, $\mu\text{mol g}^{-1} \text{h}^{-1}$	
		H ₂ O ₂	without H ₂ O ₂
VN	0.5HCOOH	759	623
VN	0.5HOOC-CH ₂ -CH(OH)-COOH (malic acid)	75	60
BN	0.05H ₂ C ₂ O ₄	489	315
SiN	0.5HCOOH	201	386
TiN	0.5HCOOH	145	228

favor of the heterogeneous photocatalysis. This may be associated with the presence of semiconductor phases with close E_g values (3.1–3.4 eV) in the ceramic matrix.

It was interesting to evaluate how the photo-Fenton process influences the rate of the evolution of molecular H₂ from organic substances under the conditions of visible irradiation in the presence of iron–ceramic composites. To this end, we performed a photocatalytic experiment on H₂ evolution from carboxylic acids in the presence of composites with the addition of H₂O₂ and without it (Table 3). The presence of H₂O₂ influences the efficiency of the photocatalytic generation of H₂ from carboxylic acids ambiguously. For the composites with high iron content (VN, BN), the addition of H₂O₂ appreciably increases the H₂ evolution rate, suggesting the role of homogeneous catalysis involving the photo-Fenton reaction. On the contrary, when using composites with low iron content (SiN, TiN), the presence of H₂O₂ decreases the production of molecular hydrogen. Probably, H₂O₂ as an electron acceptor competes for the electrons of the catalyst conduction band and decreases the H₂ generation efficiency. These relationships confirm the participation of the composites in the H₂ generation by the mechanism of heterogeneous photocatalysis.

CONCLUSIONS

Iron-containing metal–ceramic composites based on nitrides, obtained under the conditions of autowave combustion, are promising photocatalysts for the generation of molecular hydrogen from organic compounds under visible irradiation. The catalyst performance is due to the presence of semiconductor compounds and iron metal phase in the ceramic matrix, opening the possibility of combining the heterogeneous and homogeneous photocatalysis in the presence of H₂O₂. The highest catalyst performance (700–1000 $\mu\text{mol g}^{-1} \text{h}^{-1}$) is observed

when generating H₂ from oxalic acid solutions with the addition of H₂O₂. In the presence of the composite based on vanadium nitride, containing a large amount of iron, the efficiency of the H₂ release from H₂C₂O₄ under visible irradiation is considerably higher than under UV irradiation, which is caused by high photoactivity of the formed ferrioxalate complex $[\text{Fe}(\text{C}_2\text{O}_4)_3]^{3-}$ in the range 400–500 nm. High efficiency of the photocatalytic generation of H₂ in the presence of the SiN composite under visible irradiation (range 450–600 nm) is associated with the presence of the semiconductor SiC phase (band gap 2.4 eV) in the ceramic matrix.

FUNDING

The study was performed within the framework of the government assignment for the Tomsk Scientific Center, Siberian Branch, Russian Academy of Sciences (no. 0365-2019-0005) and of the research project supported by the Program for Increasing the Competitiveness of the Tomsk State University.

CONFLICT OF INTEREST

The authors declare that they have no conflict of interest.

REFERENCES

- Mansurov, R.R., Safronov, A.P., Samatov, O.V., Beketov, I.V., Medvedev, A.I., and Lakiza, N.V., *Russ. J. Appl. Chem.*, 2017, vol. 90, no. 10, pp. 1712–1721. <https://doi.org/10.1134/S1070427217100238>
- Kumaravel, V., Mathew, S., Bartlett, J., and Pillai, S.C., *Appl. Catal. B: Environmental*, 2019, vol. 244, pp. 1021–1064. <https://doi.org/10.1016/j.apcatb.2018.11.080>
- Jamali-Sheini, F., Cheraghizade, M., and Heshmatynezhad, L., *Semicond. Sci. Technol.*, 2019, vol. 34, 045008.

- <https://doi.org/10.1088/1361-6641/ab0723>
4. Jamali-Sheini, F., Cheraghizade, M., and Yousefi, R., *Solid State Sci.*, 2018, vol. 79, pp. 30–37.
<https://doi.org/10.1016/j.solidstatesciences.2018.03.005>
5. Markovskaya, D.V., Kozlova, E.A., Stonkus, O.A., Saraev, A.A., Cherepanova, S.V., and Parmon, V.N., *Int. J. Hydrogen Energy*, 2017, vol. 42, no. 51, pp. 30067–30075.
<https://doi.org/10.1016/j.ijhydene.2017.10.104>
6. Acar, C., Dincer, I., and Naterer, G.F., *Int. J. Energy Res.*, 2016, vol. 40, no. 11, pp. 1449–1473.
<https://doi.org/10.1002/er.3549>
7. Skvortsova, L.N., Batalova, V.N., Chuklomina, L.N., and Mokrousov, G.M., *Russ. J. Appl. Chem.*, 2014, vol. 87, no. 5, pp. 561–566.
<https://doi.org/10.1134/S1070427214030048>
8. Skvortsova, L.N., Batalova, V.N., Bolgaru, K.A., Artyukh, I.A., and Reger, A.A., *Russ. J. Appl. Chem.*, 2019, vol. 92, no. 1, pp. 159–165.
- <https://doi.org/10.1134/S10704272190100221>
9. *Nitride Ceramics. Combustion Synthesis, Properties, and Applications*, Gromov, A.A. and Chukhlomina, L.N., Eds., New York: Wiley–VCH, 2014.
10. Batalova, V.N., Skvortsova, L.N., Naumova, L.B., and Mateiko, I.O., *Vestn. Tomsk. Gos. Univ.*, 2013, no. 366, pp. 197–200.
11. Bacardit, J., Stotzner, J., and Chamarro, E., *Ind. Eng. Chem. Res.*, 2007, vol. 46, no. 23, pp. 7615–7619.
12. Wadley, S. and Waite, T.D., *Fenton Processes—Advanced Oxidation Processes for Water and Wastewater Treatment*, London: IWA, 2004, pp. 111–135.
13. Hislop, K.A. and Bolton, J.R., *Environ. Sci. Technol.*, 1999, vol. 33, no. 18, pp. 3119–3126.
14. Makhotkina, O.A., Kuznetsova, E.V., Matvienko, L.G., and Parmon, V.N., *Katal. Prom-sti.*, 2006, no. 4, pp. 30–37.
15. Allmand, A.J. and Reeve, L.J., *J. Chem. Soc.*, 1926, vol. 129, pp. 2852–2863.